Alexander Crain (NRC), Eldrich Rebello (WEICan),
Adam Sherwood (NRC), and Darren Jang (NRC)

Development of a NARX State-of-Charge Predictor based on Active Power Demand

Abstract

A simple neural network state-of-charge predictor trained on one-year of energy storage system data is presented. The model uses the active power command and the state-of-charge for the current time-step, and implements a nonlinear auto-regressive network with exogenous inputs to predict the state-of-charge at the subsequent time-step. The neural network training algorithm is written in the Julia programming language, independent of any existing machine learning platforms; the resulting model is compared to one developed using Python/TensorFlow. The simulation performance was validated with data collected from the energy storage system that was dispatched to follow a standard frequency regulation duty cycle not used as part of the training data. The mean-absolute-error between the predicted state of charge and the validation data is shown to be less then 1%, despite the limited data and lack of physical information about the system.

Introduction

The changing electrical grid as a result of the integration of renewable resources such as wind and solar has created a need for energy storage systems (ESS) to help balance supply and demand of energy. As a result of this growth, the development of precise yet computationally efficient ESS models for long and short term state-of-charge (SOC) and state-of-health (SOH) prediction has become necessary.

The Wind Energy Institute of Canada's (WEICan) – Figure 1 – has a 10 MW wind farm, which use a Tesla PowerPack 2 to supply the wind turbines' parasitic electrical loads. WEICan does not possess any models for their ESS – which could be used for predicting the impact of varying loads on their ESS – and are also limited in the data they can collect for the development of such a model.

Thus, this work had two goals: (1) to develop a predictive model for SOC using the very limited data available from the ESS energy management controller, and (2) to demonstrate clearly how one can program and train their own predictive neural network (NN) model without relying on existing platforms.

Figure 1. WEICan facility and wind farm

Method

This work can be sub-divided into two main categories: the hardware and the software.

Hardware Overview:

The data used in this paper was gathered from WEICan's Tesla PowerPack 2 unit. This unit is rated at 111.5 KVA with 223 kWh of energy storage capacity, and is temperature controlled. WEICan collect data using a dedicated energy meter connected to the AC output of the ESS.

This meter provides currents, voltages, phase angles, power, and energy. All meter data is logged at 1 Hz. WEICan also log data via Tesla's storage management controller (SMC), which reports battery parameters such as the state of energy, available energy, and any active errors. Data from Tesla's SMC is logged every 10 seconds. The SOC is calculated by WEICan using the state of energy parameter. It should be noted that, to ensure the ESS remains healthy, the available energy represents a corrected value where at 0% the ESS is not empty, nor is it full at 100%. The state of energy may also be adjusted by the SMC during recalibration of the ESS. However, no major recalibrations were noted in the data used for the development of the model.

Software Overview:

The NN training code was developed from scratch in the Julia programming language. The input to the model is the active power at a given time-step and the SOC at the previous time-step. The model then predicts the SOC at the next time-step. The initial SOC is set to be the first point in each training set, and active power is taken from the data directly for each point. The model knows nothing about the inner workings of the ESS or inverter, and thus is expected to include all losses in the system. This model structure is shown in Figure 2 and shows the NN contains two hidden layers with 32 nodes. Selection of the number of layers and nodes, as well as the activation functions, was done incrementally by increasing both gradually and assessing the impact on the training and validation cost curves.

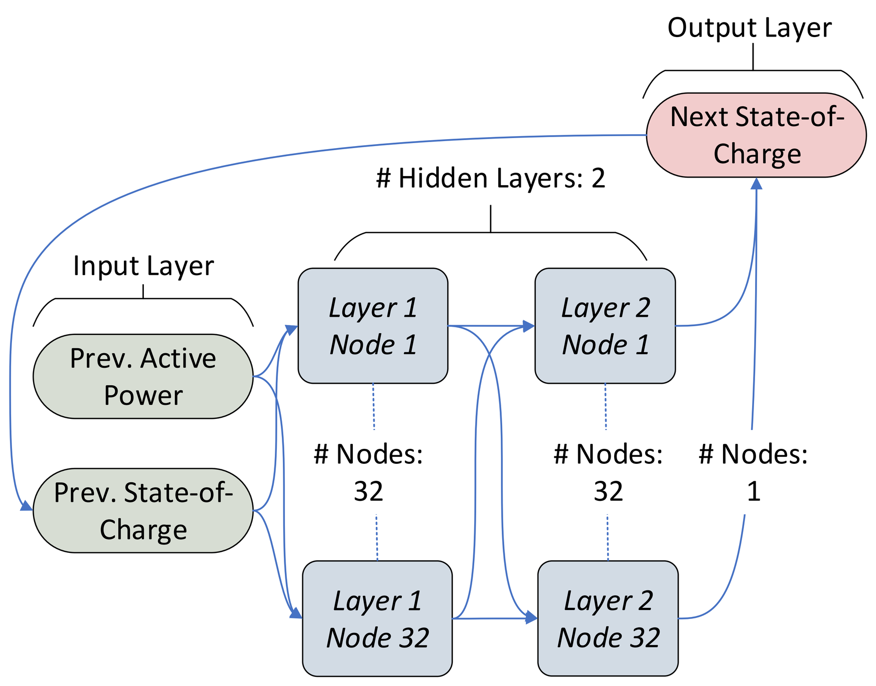

Figure 2. Neural network layout

A complete description of the code is available in the paper published alongside this poster.

Data Cleaning:

A total of 12 months of data from the WEICan ESS was used in this paper. The data was collected from May 2021 to April 2022 and was collected at a rate of 0.2 Hz. This resulted in a total of 5 760 000 raw data points per parameter. In order to use the data for training, some data cleaning was required.

The ESS data logger uses various keywords to indicate various types of bad data. These keywords were replaced with **NaNs**. Each NaN was replaced with an interpolated value. The array was then reshaped to have dimensions of **time-step, training set, and parameter**. Each data packet within each set was 256 data samples long.

The final data set containing all data was of size (256, 22500, 2); thus, the set contained 22 500 data packets, with 2 parameters and 256 data samples (per parameter) in each packet. Of the 11 520 000 data points, 65 340 were replaced by interpolated values (0.57%).

Data Exploration:

Given the simple two-input one-output data set, data exploration can be accomplished via a simple scatter plot, as shown in Figure 3. This figure shows that there is a good amount of data across the operational range of the ESS for the variables of consideration.

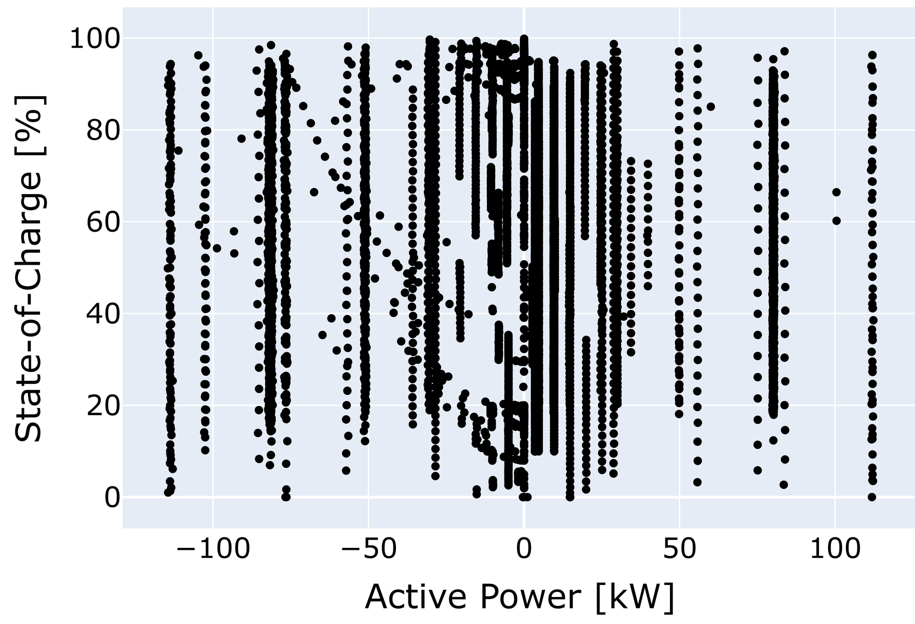

Figure 3. Data exploration

Table 1 shows the extrema and median values for the variables of interest and shows that the data set covers a large part of the ESS operational envelope.

Table 1. Statistics for data set

Channel	Maximum	Minimum	Median
Active power [kW]	112.56	-114.75	0.03
State-of-Charge [%]	99.86	0.0	77.39

Training Results:

The WEICan data set was then split randomly into training (70%), validation (15%), and testing (15%) sets. Each set was then divided into the input and output arrays: the input array contained the active power from index (1:end-1,:,:), and the output array contained the SOC from index (2:end,:,:). Data was then scaled according to the minimum and maximum values in Table 1.

After 3500 epochs, the training cost decreased from an initial value of 2309 to 42 and the validation cost decreased from an initial value of 832 to 18. The training and validation curves are shown in Figure 4. The initially high cost decreases rapidly in the first 100 epochs, and is not shown in Figure 4. The training and validation curves both show good convergence, indicating that it is unlikely the model was over-trained.

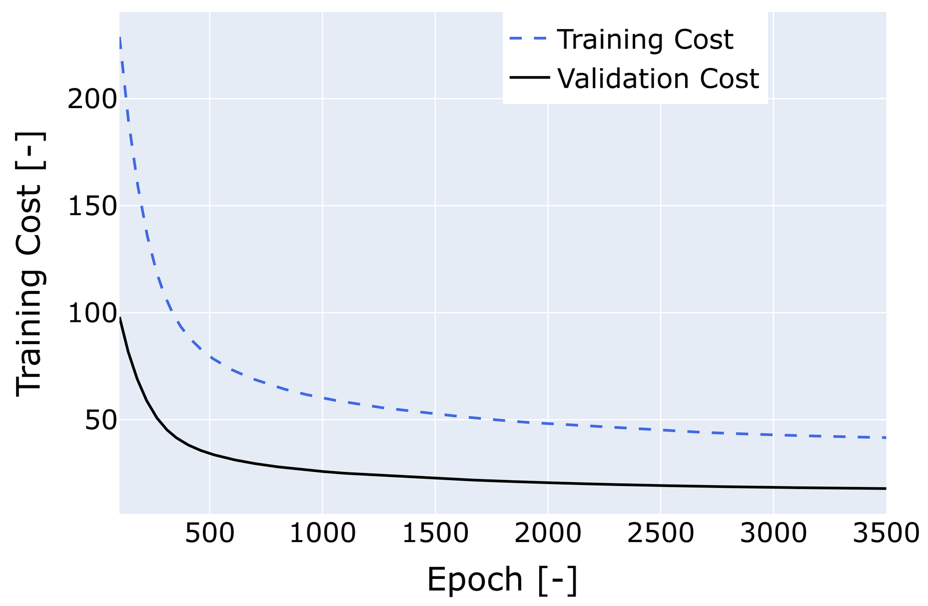

Figure 4. Training and validation curves

Model Validation:

To validate the model, the ESS was subjected to the standard frequency regulation duty cycle in Figure 5.

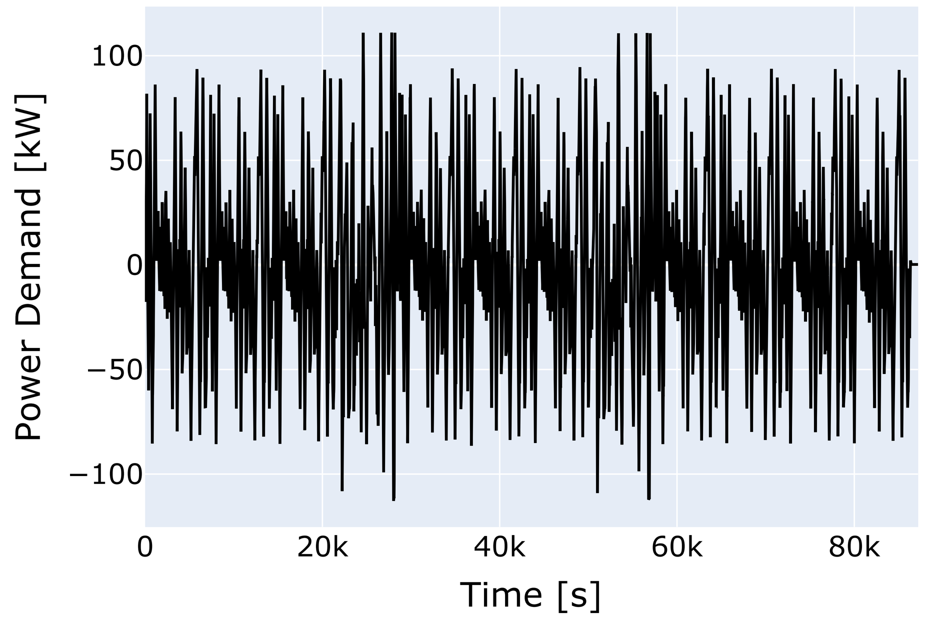

Figure 5. Frequency regulation duty cycle

The ESS was subjected to the frequency regulation load cycle from July 19-20, 2022. Active power and initial SOC were collected and used as inputs into both NARX models for validation; the results are shown in Figure 6. The mean-absolute-error between the data and the Julia model is 0.53%, the absolute maximum error is 3.03%, and the median error is 0.29%.

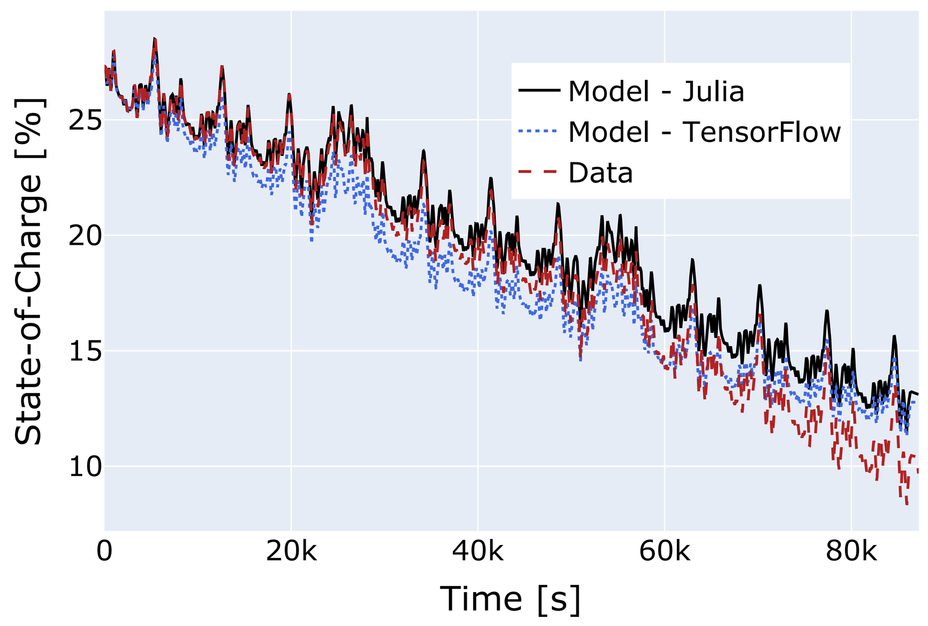

Figure 6. Model validation results

Conclusion

Ultimately, a simple NARX was developed for the prediction of state-of-charge for a black-box ESS using active power and the previous state-of-charge as the inputs for each prediction. The largest deviations from the experiment in the Julia model occur during the high-power portions of the duty cycle (20k-30k seconds and 50k-60k seconds). This may be due to the lack of training data in those regions. Future work on this model will involve collecting additional data at higher power, as well as the development of a state-of-health monitor in the form of a discriminator network, which would be trained in parallel with the generator network presented in this research.

Partners

Wind Energy Institute of Canada
Institut de l'énergie éolienne du Canada

The authors acknowledge the support of NRCan OERD and the EME Advanced Clean Energy Program.